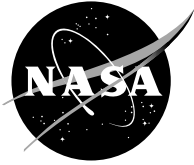


NASA/TM—2002-211718



Preliminary Study on Fatigue Strengths of Fretted Ti-48Al-2Cr-2Nb

Kazuhisa Miyoshi, Bradley A. Lerch, and Susan L. Draper
Glenn Research Center, Cleveland, Ohio

August 2002

The NASA STI Program Office . . . in Profile

Since its founding, NASA has been dedicated to the advancement of aeronautics and space science. The NASA Scientific and Technical Information (STI) Program Office plays a key part in helping NASA maintain this important role.

The NASA STI Program Office is operated by Langley Research Center, the Lead Center for NASA's scientific and technical information. The NASA STI Program Office provides access to the NASA STI Database, the largest collection of aeronautical and space science STI in the world. The Program Office is also NASA's institutional mechanism for disseminating the results of its research and development activities. These results are published by NASA in the NASA STI Report Series, which includes the following report types:

- **TECHNICAL PUBLICATION.** Reports of completed research or a major significant phase of research that present the results of NASA programs and include extensive data or theoretical analysis. Includes compilations of significant scientific and technical data and information deemed to be of continuing reference value. NASA's counterpart of peer-reviewed formal professional papers but has less stringent limitations on manuscript length and extent of graphic presentations.
- **TECHNICAL MEMORANDUM.** Scientific and technical findings that are preliminary or of specialized interest, e.g., quick release reports, working papers, and bibliographies that contain minimal annotation. Does not contain extensive analysis.
- **CONTRACTOR REPORT.** Scientific and technical findings by NASA-sponsored contractors and grantees.

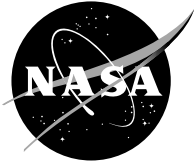
- **CONFERENCE PUBLICATION.** Collected papers from scientific and technical conferences, symposia, seminars, or other meetings sponsored or cosponsored by NASA.
- **SPECIAL PUBLICATION.** Scientific, technical, or historical information from NASA programs, projects, and missions, often concerned with subjects having substantial public interest.
- **TECHNICAL TRANSLATION.** English-language translations of foreign scientific and technical material pertinent to NASA's mission.

Specialized services that complement the STI Program Office's diverse offerings include creating custom thesauri, building customized data bases, organizing and publishing research results . . . even providing videos.

For more information about the NASA STI Program Office, see the following:

- Access the NASA STI Program Home Page at <http://www.sti.nasa.gov>
- E-mail your question via the Internet to help@sti.nasa.gov
- Fax your question to the NASA Access Help Desk at 301-621-0134
- Telephone the NASA Access Help Desk at 301-621-0390
- Write to:
NASA Access Help Desk
NASA Center for Aerospace Information
7121 Standard Drive
Hanover, MD 21076

NASA/TM—2002-211718



Preliminary Study on Fatigue Strengths of Fretted Ti-48Al-2Cr-2Nb

Kazuhisa Miyoshi, Bradley A. Lerch, and Susan L. Draper
Glenn Research Center, Cleveland, Ohio

National Aeronautics and
Space Administration

Glenn Research Center

August 2002

The Aerospace Propulsion and Power Program at
NASA Glenn Research Center sponsored this work.

Available from

NASA Center for Aerospace Information
7121 Standard Drive
Hanover, MD 21076

National Technical Information Service
5285 Port Royal Road
Springfield, VA 22100

Available electronically at <http://gltrs.grc.nasa.gov/GLTRS>

Preliminary Study on Fatigue Strengths of Fretted Ti-48Al-2Cr-2Nb

Kazuhisa Miyoshi, Bradley A. Lerch, and Susan L. Draper
National Aeronautics and Space Administration
Glenn Research Center
Cleveland, Ohio 44135

Abstract

The fatigue behavior (stress-life curve) of gamma titanium aluminide (Ti-48Al-2Cr-2Nb, atomic percent) was examined by conducting two tests: first, a fretting wear test with a fatigue specimen in contact with a typical nickel-based superalloy contact pad in air at temperatures of 296 and 823 K and second, a high-cycle fatigue test of the prefretted Ti-48Al-2Cr-2Nb fatigue specimen at 923 K. Reference high-cycle fatigue tests were also conducted with unfretted Ti-48Al-2Cr-2Nb specimens at 923 K. All Ti-48Al-2Cr-2Nb fatigue specimens were machined from cast slabs. The results indicate that the stress-life results for the fretted Ti-48Al-2Cr-2Nb specimens exhibited a behavior similar to those of the unfretted Ti-48Al-2Cr-2Nb specimens. The values of maximum stress and life for the fretted specimens were almost the same as those for the unfretted specimens. The resultant stress-life curve for the unfretted fatigue specimens was very flat. The flat appearance in the stress-life curve of the unfretted specimens is attributed to the presence of a high density of casting pores. The fatigue strengths of both the fretted and unfretted specimens can be significantly affected by the presence of this porosity, which can decrease the fatigue life of Ti-48Al-2Cr-2Nb. The presence of the porosity made discerning the effect of fretting damage on fatigue strength and life of the specimens difficult.

Introduction

Fretting failure can occur in a variety of engine components (refs. 1 and 2). The most damaging effect of fretting is the significant reduction in fatigue-resistance of the fretted component even with mild wear. This form of damage arises when the contacting surfaces undergo oscillatory displacement of small amplitude. As a result of the displacement, adhering metal particles are produced (adhesive wear), which can oxidize. These oxidized particles are abrasive, subsequently causing abrasive wear (a severe form of wear) of the surfaces. The failure probability of engine components abruptly increases at this stage. Progressive fretting produces galling, which in turn can cause premature fatigue crack initiation. Propagation of such cracks under cyclic loads may result in the failure of the blade or disk and convey fragments into the engine with catastrophic results. Even a small tribological failure can clearly lead to catastrophic results (ref. 3).

The material of interest in this study is gamma titanium aluminide (γ -TiAl). This material has potential applications for low-pressure turbine blades. A concern for the γ -TiAl blades is fretting at the dovetail caused by alternating centrifugal force and a natural high-frequency blade vibration (fig. 1). For example, observations of service-exposed Ti-based alloy fan blade-disk couples in fan engine propulsion systems revealed the presence of severe fretting fatigue damage on the contacting surfaces of blade dovetails and disk slots (ref. 3).

The objective of this preliminary study was to evaluate the effects of fretting on the fatigue-resistance of γ -TiAl (Ti-48Al-2Cr-2Nb, atomic percent). Ti-48Al-2Cr-2Nb fatigue specimens were machined from cast slabs. Two tests, a fretting test and a fatigue test, were conducted with the Ti-48Al-2Cr-2Nb fatigue specimens. First, baseline-fretting tests were conducted with a Ti-48Al-2Cr-2Nb fatigue specimen in contact with a typical, aged nickel-based superalloy contact pad in air at temperatures of 296 and 823 K using

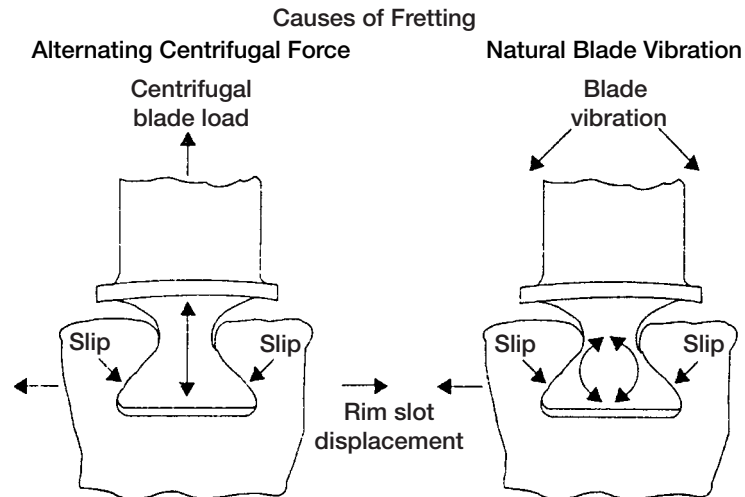


Figure 1.—Fan and compressor blade dovetail displacements.

a fretting apparatus. Second, fatigue tests in air at 923 K using a high-cycle fatigue test setup were separately conducted with the prefretted fatigue specimens. Reference fatigue tests were also conducted with unfretted Ti-48Al-2Cr-2Nb fatigue specimens in air at 923 K.

Materials

The Ti-48Al-2Cr-2Nb specimens were determined to be of the following composition (in atomic percent): titanium, 47.9; aluminum, 48.0; niobium, 1.96; chromium, 1.94; carbon, 0.013; nitrogen, 0.014; and oxygen, 0.167 (ref. 4).

Specimens and Tests

Specimens.—All Ti-48Al-2Cr-2Nb fatigue specimens were machined from cast slabs. Each fatigue specimen (fig. 2) had a total length of 152.4 mm (6 inches) with rectangular (2.03 mm × 12.70 mm) cross section ends and a straight gage section, 25.9 mm long. The specimens had an elliptical cross section in the gage. The average surface roughness, R_a , and Vickers hardness for the Ti-48Al-2Cr-2Nb fatigue specimens are summarized in table 1. Figure 3(a) presents a three-dimensional, optical interferometry image of the gage section of the fatigue specimen. The surface shows a relatively homogeneous surface texture containing machined grooves along the length of the specimen in the direction of the fatigue loading. The mean value of centerline average roughness, R_a , measured parallel to the length of the specimen is 0.57 μm with a standard deviation of 0.17 μm . The R_a measured perpendicular to the length of the specimen is 0.75 μm with a standard deviation of 0.10 mm. However, the detailed optical interferometry image shows a large casting pore with a length as large as 70 μm (fig. 3(b)). The Ti-48Al-2Cr-2Nb fatigue specimen generally contained cavities with depths of 2 to 4 μm and cutting grooves with depths of 3 μm . Therefore, the maximum height (peak-to-valley) of the surface, R_t , was relatively large, having a value of 8.8 μm and a standard deviation of 2.2 μm . Note that R_t is the vertical distance between the highest (R_p) and lowest (R_v) points as calculated over the entire measured surface. It is defined as: $R_t = R_p + R_v$. The maximum profile peak height R_p is the distance between the highest point of the surface and the mean surface for the entire measured surface. The maximum profile valley depth R_v is the distance between the lowest point of the surface and the mean surface for the entire measured surface.

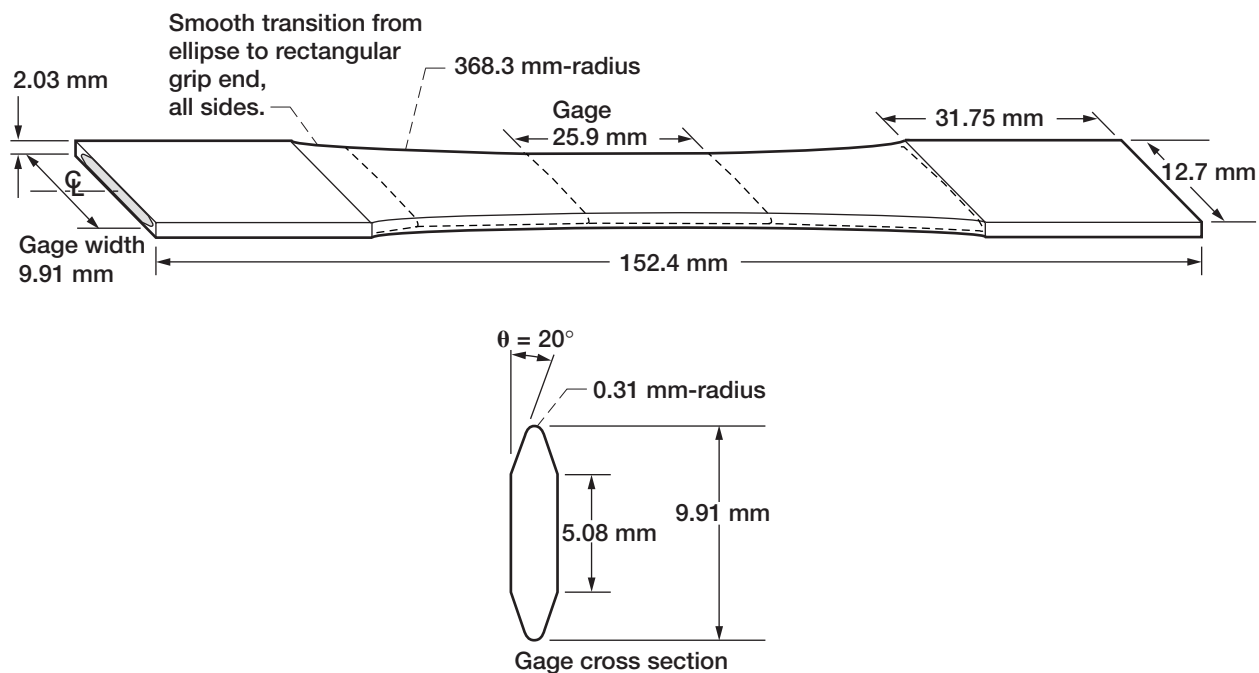


Figure 2.—Ti-48Al-2Cr-2Nb fatigue specimen.

TABLE 1.—SURFACE ROUGHNESS AND VICKERS HARDNESS OF SPECIMENS

Specimen	Centerline-average roughness, R_a , nm		Vickers hardness, H_v , GPa	
	Mean	Standard deviation	Mean	Standard deviation
Ti-48Al-2Cr-2Nb fatigue specimen	370	49	3.78	0.57
9.4-mm-diameter, hemispherical, nickel-based superalloy pin	40	8.9	5.52	0.44
Nickel-based superalloy contact pad: two-sided wedge with a 12-mm-long knife-edge	2.75×10^3	65	4.85	0.28
Nickel-based superalloy contact pad: wedgelike shape with rectangular flat	419	42	4.78	0.21

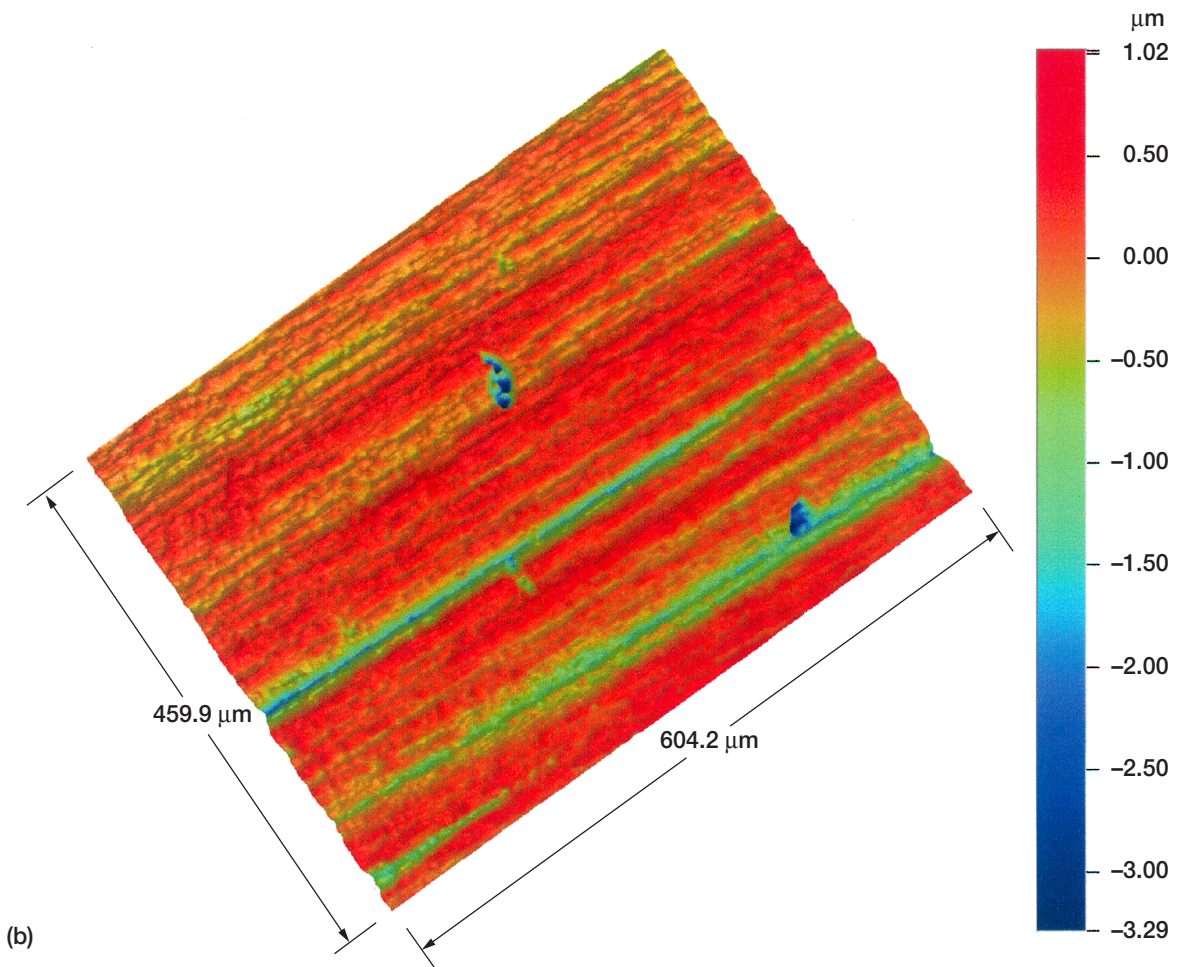
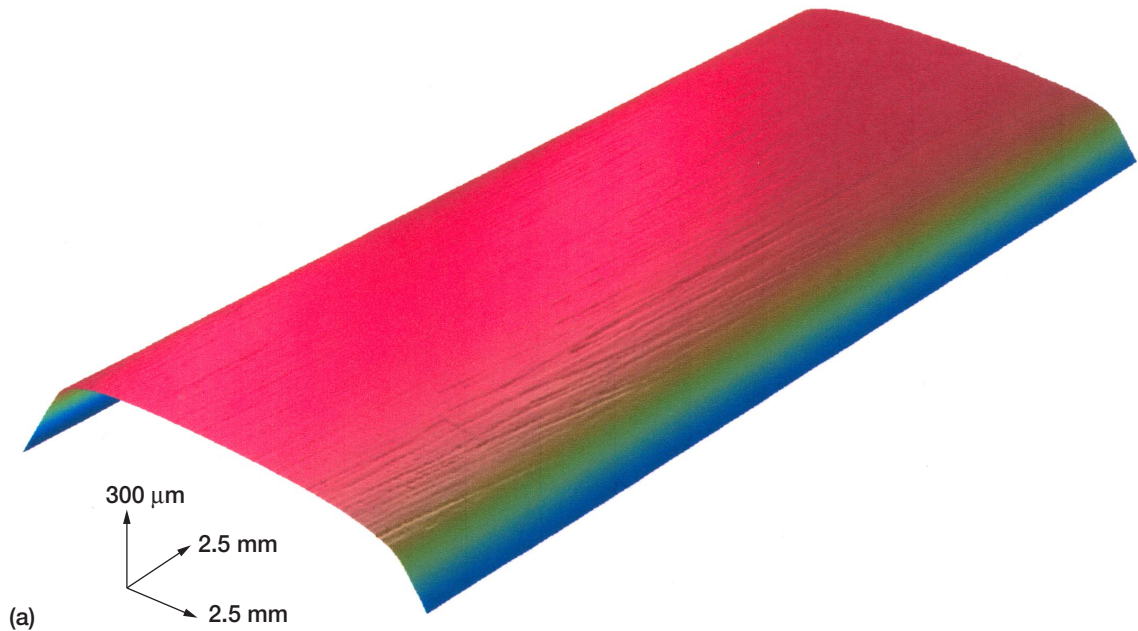


Figure 3.—Three-dimensional, optical interferometry image of gage section of machined Ti-48Al-2Cr-2Nb fatigue specimen. (a) Overview showing a homogeneous surface texture with grooves. (b) Casting porosity.

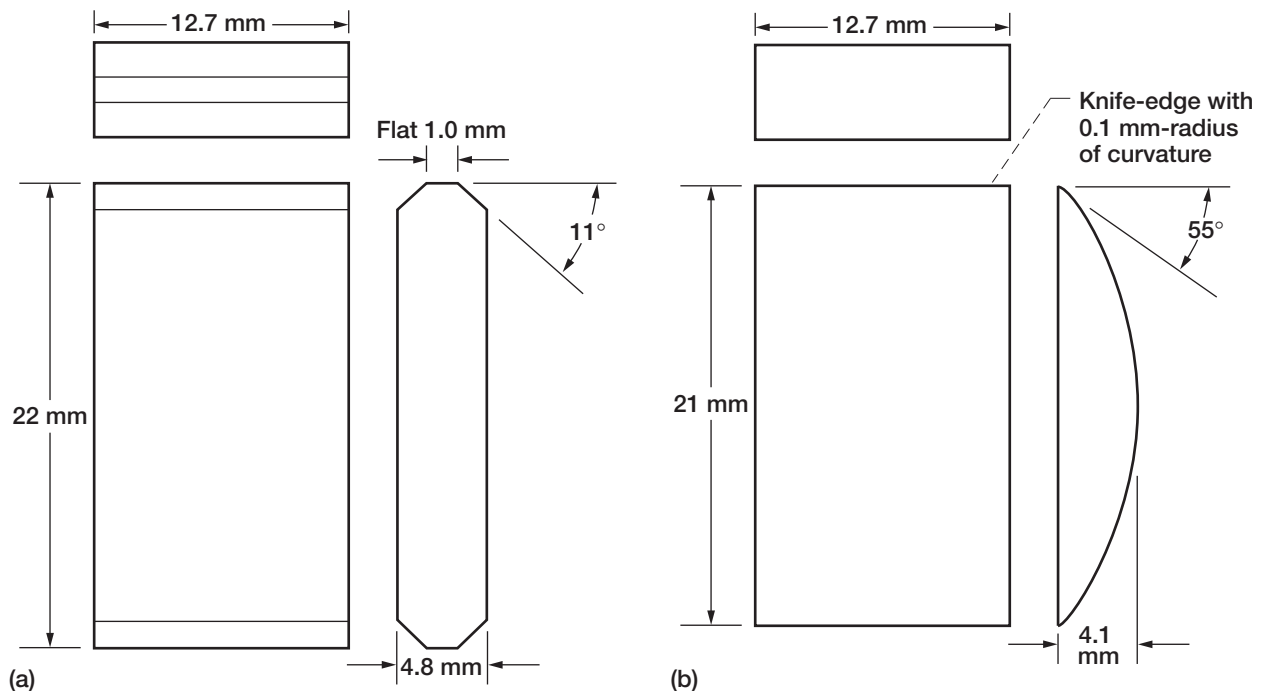


Figure 4.—Nickel-based superalloy contact pads. (a) Wedge-like pad with flat. (b) Wedge with knife-edge.

There were three types of nickel-based superalloy contact pads. One (fig. 4(a)) had a wedgelike shape with two rectangular flats (1.00 mm × 12.70 mm) and one of the rectangular-shaped flats was brought into contact with the Ti-48Al-2Cr-2Nb fatigue specimen (fig. 5(a)). The second (fig. 4(b)) was a two-sided wedge with 12.70 mm long knife-edges. The contained angle between the two sides was 35° and the average radius of curvature for the knife-edge was less than 0.1 mm (fig. 4(b)). One of the knife-edges was brought into contact with the Ti-48Al-2Cr-2Nb fatigue specimen, as schematically shown in fig. 5(b). The third was a 9.4-mm-diameter hemispherical pin (not shown in the figure). The spherical surface was brought into contact with the Ti-48Al-2Cr-2Nb fatigue specimen. The average surface roughness, Ra, and Vickers hardness for the nickel-based superalloy contact pads (including pins) are also summarized in table 1.

Fretting Test.—The fretting apparatus used in this investigation was basically the same as that shown in fig. 6. Fretting experiments were conducted with aged nickel-based superalloy pads in contact with Ti-48Al-2Cr-2Nb fatigue specimens (fig. 5). The Ti-48Al-2Cr-2Nb fatigue specimen was placed on a rectangular parallelepiped, strip heater (127 mm × 16 mm × 6.4 mm) and was held by four clamps (6.4 mm × 12.7 mm × 2.0 mm), as shown in figure 5.

All fretting wear experiments were conducted under the conditions shown in table 2(a) to (d). Both nickel-based superalloy contact pads and Ti-48Al-2Cr-2Nb fatigue specimens were rinsed with 200-proof ethyl alcohol before installation in the fretting apparatus.

Fatigue Test.—Both prefretted Ti-48Al-2Cr-2Nb fatigue specimens and unfretted Ti-48Al-2Cr-2Nb fatigue specimens were tested in high-cycle fatigue at 923 K and at a frequency of 80 Hz. Based on previous experience, the fatigue-crack growth rates are highest at 923 K (650 °C) for Ti-48Al-2Cr-2Nb (ref. 5), and therefore this temperature was chosen for testing to simulate the worst-case scenario. Fatigue tests were all run with a load ratio R of 0.05 ($R = \sigma_{\min} / \sigma_{\max}$). Due to the flat nature of the S-N (stress vs. cycles to failure) curve for γ -TiAl, step fatigue tests (refs. 6 and 7) were used to determine the maximum fatigue strength for prefretted Ti-48Al-2Cr-2Nb fatigue specimens. Based on the previous experience,

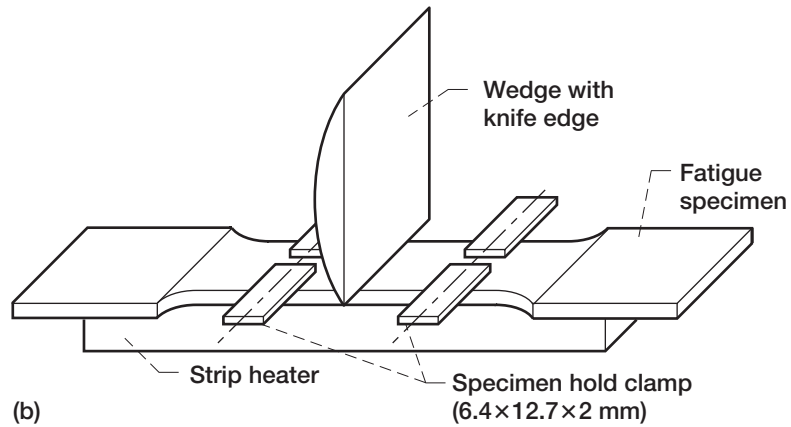
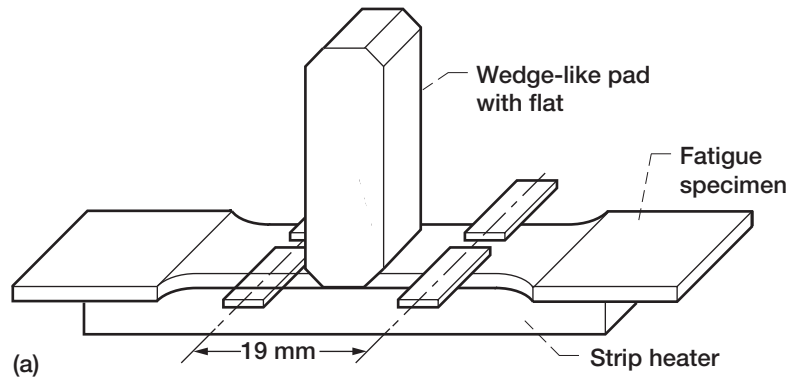


Figure 5.—Fatigue specimen and contact configuration. (a) Wedge-like pad with flat on fatigue specimen. (b) Wedge with knife-edge on fatigue specimen.

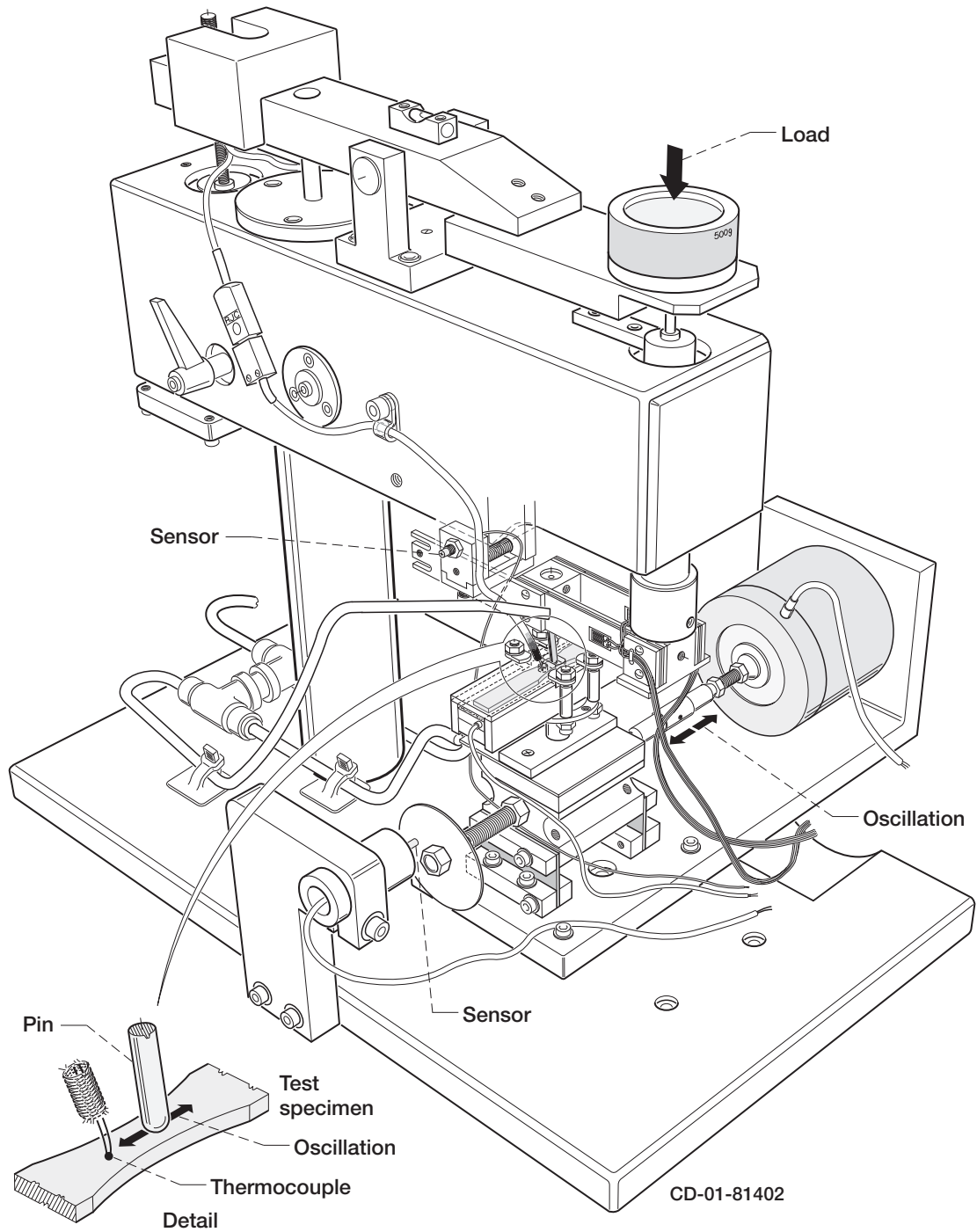


Figure 6.—Fretting apparatus.

TABLE 2.—FRETTING TEST CONDITIONS

(a) Fretting with spherical superalloy pin specimens.

(a.1) Fretting conditions on both front and back sides of fatigue specimen (I.D. No. 063-03-3).

9.4-mm-diameter spherical pin specimen	Superalloy
Flat specimen	γ -TiAl, Specimen I.D. No. 063-03-3
Environment	Air at 296 K
Load	1.5 N for first 600 000 cycles and subsequently 3.0 N for 7 million cycles
Frequency	Hz: 81
Amplitude	50 μ m
Total number of cycles	7 million
Fretting direction	Parallel to the length of the fatigue specimen (in the direction of the fatigue loading)

(b) Fretting at 823 K.

(b.1) Fretting on front side of fatigue specimen (I.D. No. 6-3-3).

Knife-edge-shaped contact pad specimen	Superalloy
Fatigue specimen	γ -TiAl, Specimen I.D.: 6-3-3
Environment	Air at 823 K
Load	1.5-3.0 N
Amplitude (mean value)	50 μ m
Frequency	80 Hz and 160 Hz
Number of cycles	20 million cycles at 80 Hz and subsequent 80 million cycles at 160 Hz
Total number of cycles	100 million cycles
Fretting direction	Perpendicular to the length of the fatigue specimen (perpendicular to the direction of the fatigue loading)

(b.2) Fretting on back side of fatigue specimen (I.D. No. 6-3-3).

Knife-edge-shaped contact pad specimen	Superalloy
Fatigue specimen:	γ -TiAl, Specimen I.D.: 6-3-3
Environment	Air at 823 K
Load	1.5-3.0 N
Amplitude (mean value)	50 μ m
Frequency	80 Hz
Number of cycles	40 million cycles at 80 Hz
Total number of cycles	40 million cycles
Fretting direction	Perpendicular to the length of the fatigue specimen (perpendicular to the direction of the fatigue loading)

TABLE 2.—(CONTINUED).

(c) Fretting at different temperatures.

(c.1) Fretting on front side of fatigue specimen (I.D. No. 5-1-3).

Knife-edge-shaped contact pad specimen	Superalloy
Fatigue specimen	γ -TiAl, Specimen I.D. No. 5-1-3
Environment	Air at 823 K and at room temperature
Load	1.5-3.0 N
Amplitude (mean value)	50 μ m
Frequency	160 Hz
Number of cycles	36 million cycles at 823 K and subsequently 73 million cycles at 296 K
Total number of cycles	109 million cycles
Fretting direction	Parallel to the length of the fatigue specimen (in the direction of the fatigue loading)

(c.2) Fretting on back side of fatigue specimen (I.D. No. 5-1-3).

Knife-edge-shaped contact pad specimen	Superalloy
Fatigue specimen:	γ -TiAl, Specimen I.D. No. 5-1-3
Environment	Air at 823 K and subsequently at 296 K
Load	1.5-3.0 N
Amplitude (mean value)	50 μ m
Frequency	160 Hz
Number of cycles	109 million cycles at 823 K and subsequently 42 million cycles at 296 K
Total number of cycles	151 million cycles
Fretting direction	Parallel to the length of the fatigue specimen (in the direction the fatigue loading)

TABLE 2.—(CONCLUDED)

(d) High load fretting.

(d.1) Fretting conditions on front side of fatigue specimen (I.D. No. 5-1-6).

Wedgelike contact pad specimen with rectangular flat	Superalloy
Fatigue specimen	γ -TiAl, Specimen I.D.: 5-1-6
Environment	Air at 823 K
Load	450 N
Amplitude	90 μ m
Frequency	80 Hz
Total number of fretting cycles	16 million fretting cycles at 823 K
Fretting direction	Parallel to the length of the fatigue specimen (in the direction of the fatigue loading)

(d.2) Fretting on back side of fatigue specimen (I.D. No. 5-1-6).

Wedgelike contact pad specimen with rectangular flat	Superalloy
Fatigue specimen	γ -TiAl, Specimen I.D.: 5-1-6
Environment	Air at 296 K
Load	450 N
Amplitude (mean value)	90 μ m
Frequency	80 Hz
Total number of cycles	16 million fretting cycles at 296 K
Fretting direction	Parallel to the length of the fatigue specimen (in the direction of the fatigue loading)

a starting stress level was chosen. If the specimen survived 10^6 cycles, the stress was increased by 14 MPa and run to failure or 10^6 cycles. The stress level was increased until failure (two pieces) occurred. The use of step fatigue testing avoided wasting a large number of specimens due to runouts as each specimen was forced to fail.

Results and Discussion

Observations

Fretting Wear of Superalloy.—Surface and subsurface damage always occurred on the interacting surfaces of the Ti-48Al-2Cr-2Nb and superalloy during fretting in air (ref. 4). The surface damage of the Ti-48Al-2Cr-2Nb and superalloy consisted of material transfer and back transfer, pits, oxides and debris, scratches, fretting craters and wear scars, plastic deformation, and cracks. In general the damage of Ti-48Al-2Cr-2Nb is analogous to that of superalloy. Since the observation of surface and subsurface damage of Ti-48Al-2Cr-2Nb was already reported (ref. 4), the damage of the superalloy will be primarily discussed below.

Figures 7(a) to (b) show examples of surface damage produced on superalloy: metallic wear debris of Ti-48Al-2Cr-2Nb and superalloy, oxides, scratches (grooves), small craters, plastically deformed asperities, and cracks, all of which are similar to those observed on Ti-48Al-2Cr-2Nb. The scratches (fig. 7(a)) can be caused by hard, oxidized wear particles of superalloy and Ti-48Al-2Cr-2Nb, which are trapped between the interacting surfaces or are adhered to or embedded in the counterpart Ti-48Al-2Cr-2Nb surface. In fig. 7(a) scratches and fracture pits (craters) were produced by abrasion, a severe

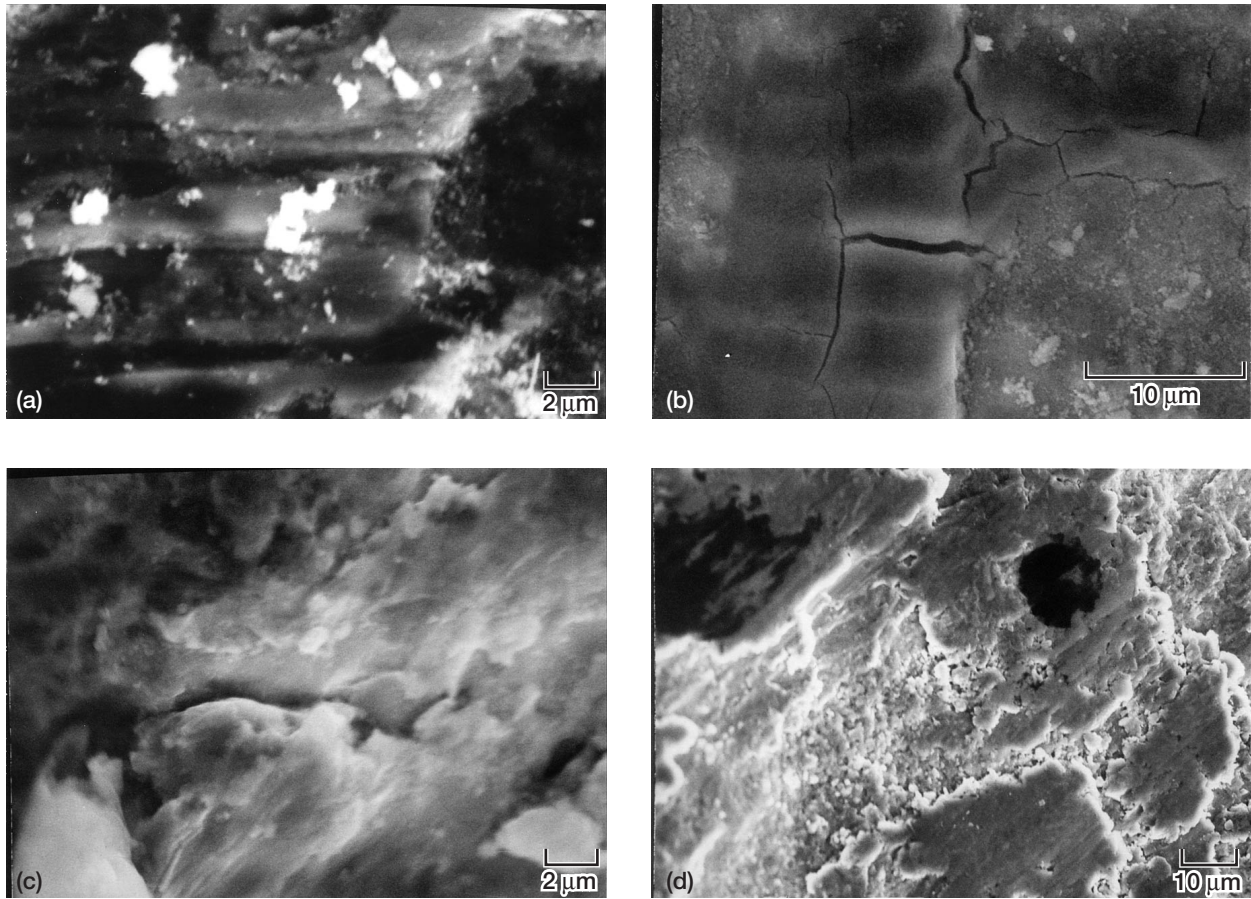


Figure 7.—Surface and subsurface damage in superalloy pin in contact with Ti-48Al-2Cr-2Nb flat. (a) Scratches. (b) Cracks in oxide layers. (c) Cracks in metal. (d) Fracture pits and plastic deformation. Fretting conditions: load, 1 N; frequency, 80 Hz; slip amplitude; 50 μm ; and total number of cycle, 1 million: environment, air: and temperature, 823 K.

form of wear. The trapped wear particles and the adhered (or embedded) wear particles plow or cut the superalloy surface. The trapped wear particles have a scratching effect on both surfaces; and because they carry part of the load, they cause concentrated pressure peaks on both surfaces (ref. 4). The pressure peaks may well be the origin of crack nucleation in the oxide layers and the bulk alloys.

Oxide layers readily form on the superalloy surfaces at 823 K and are often a favorable solution to wear problems. However, cracks occurred in the oxide layers both within and around the contact areas, as shown in fig. 7(b).

Fractures in the protective oxide layers produced cracks in the bulk superalloy (fig. 7(c)) and also produced wear debris, chemically active fresh surfaces, plastic deformation, craters, and fracture pits (fig. 7(d)). This wear debris can cause third-body abrasive wear. Local, direct contacts between the fresh surfaces of Ti-48Al-2Cr-2Nb and superalloy resulted in increased adhesion and local stresses, which may cause plastic deformation, flakelike wear debris, and craters.

Fretting Scar on Fatigue Specimen and Contact Pad.—All of the Ti-48Al-2Cr-2Nb fatigue specimens and the superalloy contact pads showed fretting damage. Typical damage observed on a Ti-48Al-2Cr-2Nb fatigue specimen at a low magnification is shown in figure 8. Because of the contact geometry, a long wear scar was produced perpendicular to the length of the fatigue specimen in the center of gauge section. In figure 8 the wear debris has been removed from the fatigue specimen surface to show the overall geometry of wear scar.

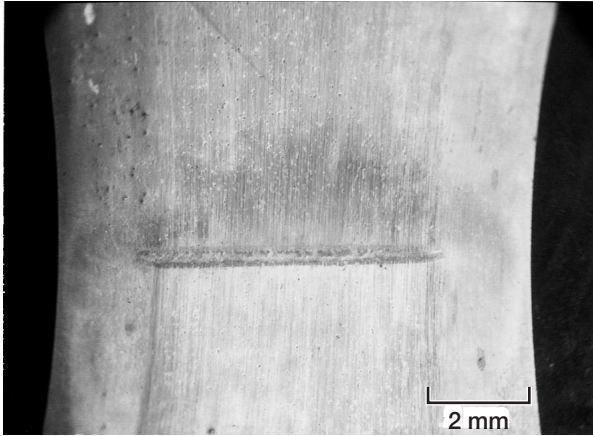


Figure 8.—Wear scar produced on Ti-48Al-2Cr-2Nb fatigue specimen in contact with superalloy contact pad. Table 2(b.2) presents the fretting conditions.



Figure 9.—Wear scar with wear debris particles produced on Ti-48Al-2Cr-2Nb fatigue specimen in contact with superalloy contact pad. Table 2(b.2) presents the fretting conditions.

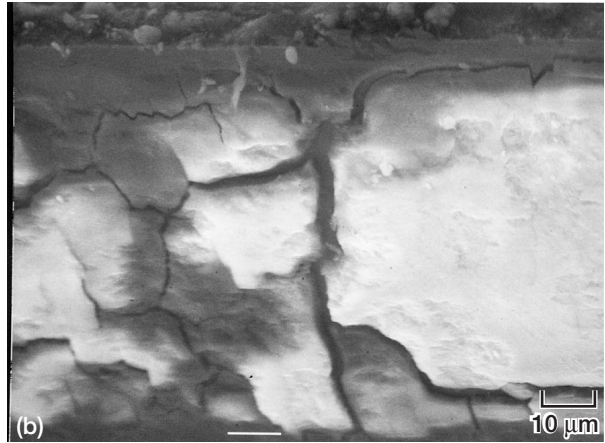
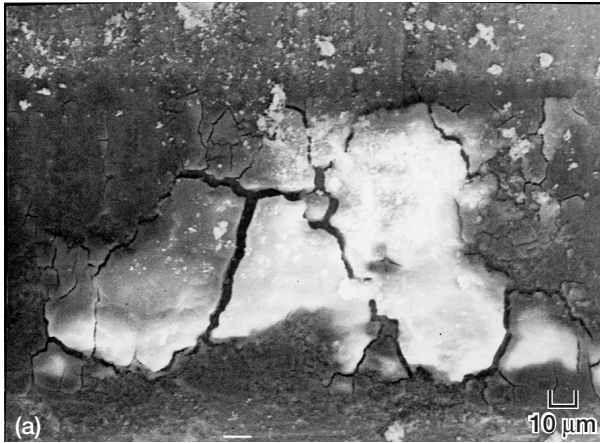


Figure 10.—Protective oxide layers produced on both (a) Ti-48Al-2Cr-2Nb fatigue specimen and (b) superalloy contact pad. Table 2(b.2) presents the fretting conditions.

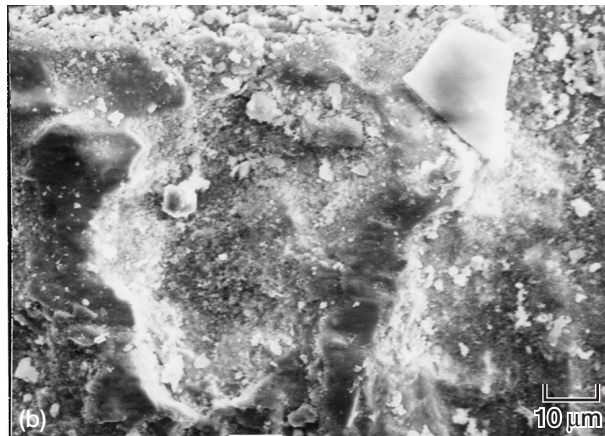


Figure 11.—Surface damages produced on both (a) Ti-48Al-2Cr-2Nb fatigue specimen and (b) superalloy contact pad. Table 2(b.2) presents the fretting conditions.

Figure 9 shows a typical example of a wear scar with wear debris from fretting produced on the Ti-48Al-2Cr-2Nb fatigue specimen in contact with the superalloy contact pad. Because of the specimen geometry, a large amount of wear debris is deposited just outside the line contact area. Pieces of the Ti-48Al-2Cr-2Nb and its oxides are generally torn out or sheared off during fretting.

Protective oxide layers readily form on both Ti-48Al-2Cr-2Nb and superalloy at 823 K in air. Although cracks occurred in the oxide layers formed on Ti-48Al-2Cr-2Nb and superalloy (figs. 10(a) and (b), respectively), the alloy surfaces were protected by these oxide layers.

On the other hand, figures 11(a) and (b) show examples of the Ti-48Al-2Cr-2Nb and superalloy surfaces that are torn out or sheared off during fretting. There are fractured pits, flakelike wear debris, and oxide wear particles in the contact areas of both Ti-48Al-2Cr-2Nb and superalloy surfaces.

Baseline Fretting Fatigue Tests

Fatigue tests were conducted with both prefretted fatigue specimens and unfretted Ti-48Al-2Cr-2Nb. These tests were conducted to determine the number of cycles to failure at each stress level, and in effect create a preliminary stress-life curve. The fatigue results for prefretted Ti-48Al-2Cr-2Nb specimens from high-cycle fatigue tests are included in table 3(a). The prefretted specimen shown in table 2(a) failed near the grip section at a maximum stress of 282 MPa at 11,200 cycles. Fretting damage (wear scars) produced by spherical superalloy pin specimens was not significant enough to cause failure. The fretted specimen shown in table 2(b) failed near the clamp section at a maximum stress of 331 MPa at 9,040 cycles. Also, the fretted specimen shown in table 2(c) failed near the clamp section at a maximum stress of 248 MPa at 6,560 cycles. Fretting damage produced by the clamps could be greater than that by the contact pads. The fretted specimen shown in table 2(d) failed near the fretted area at a maximum stress 386 MPa at 12,400 cycles.

The fatigue results for unfretted Ti-48Al-2Cr-2Nb specimens from high-cycle fatigue tests are included in table 3(b). The stress-life results for the prefretted specimens exhibited a behavior similar to those of the unfretted specimens. The values of maximum stress for the prefretted specimens were almost the same as those of the unfretted specimens.

TABLE 3.—STRESS-LIFE RESULTS

(a) Prefretted Ti-48Al-2Cr-2Nb.

Maximum stress, MPa	Number of cycles to failure	Table showing fretting conditions	Specimen I.D. number
286	11,200	2 (a)	063-3-3
331	9,040	2 (b)	6-3-3
248	6,560	2 (c)	5-1-3
386	12,400	2 (d)	5-1-6

(b) Unfretted Ti-48Al-2Cr-2Nb.

Maximum stress, MPa	Number of cycles to failure
288	5,100
266	681,400
314	7,100
346	132,000
245	947,040

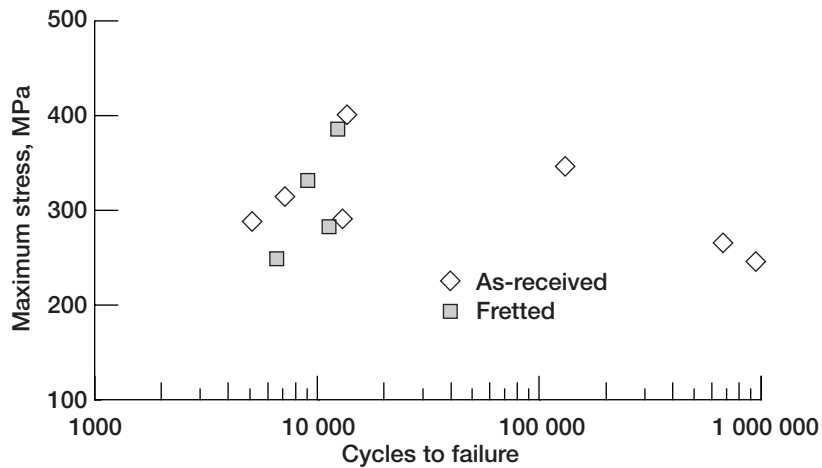


Figure 12.—Baseline fatigue test results for both fretted Ti-48Al-2Cr-2Nb fatigue specimens and as-received, unfretted Ti-48Al-2Cr-2Nb fatigue specimens.

The data from tables 3(a) and (b) are plotted in figure 12. Figure 12 appeared that the resultant stress-life curve for the unfretted fatigue specimens was very flat and exhibited a behavior similar to that of ceramic materials (refs. 8–11). Similar fretting fatigue stress-life curves have also been reported for γ -TiAl based materials (refs. 12 and 13). The flat appearance in the stress-life curve is attributed to the presence of a high density of casting pores.

Thus, the fatigue strengths of both prefretted and unfretted Ti-48Al-2Cr-2Nb fatigue specimens were significantly affected by the presence of casting pores. This porosity obscured the effect of fretting damage on fatigue strength and life of Ti-48Al-2Cr-2Nb.

Concluding Remarks

The fatigue behavior (stress-life curve) of γ -TiAl (Ti-48Al-2Cr-2Nb) was examined by conducting two tests: first, a fretting wear test with a Ti-48Al-2Cr-2Nb fatigue specimen in contact with a typical nickel-based superalloy contact pad in air at 296 and 923 K and second, a fatigue test of the fretted specimen in air at 923 K. Reference fatigue tests were also conducted with as-received, unfretted Ti-48Al-2Cr-2Nb specimens in air at 923 K. All Ti-48Al-2Cr-2Nb fatigue specimens were machined from cast slabs. As a result, the following conclusions are drawn from the data presented:

1. For both fretted fatigue and unfretted fatigue specimens, fatigue strengths can be significantly affected by the presence of casting porosity.
2. Casting porosity can obscure the effect of fretting damage on the fatigue strength of cast Ti-48Al-2Cr-2Nb. The stress-life results for the fretted specimens exhibited a behavior similar to those of the unfretted specimens. The values of maximum stress for the fretted Ti-48Al-2Cr-2Nb specimens were almost the same as those of the unfretted Ti-48Al-2Cr-2Nb specimens.
3. The resultant stress-life curve for the unfretted Ti-48Al-2Cr-2Nb fatigue specimens was very flat. The flat appearance in the stress-life curve is attributed to the presence of a high density of casting pores.

References

1. D.W. Hoepfner, V. Chandrasekaran, and C.B. Elliott III (editors), *Fretting Fatigue: Current Technology and Practices*, ASTM STP 1367, West Conshohocken, PA 19428–2959, 2000.
2. S.R. Brown (Symposium Chairman), *Materials Evaluation Under Fretting Conditions*, ASTM 780, Philadelphia, PA 19103, 1982.
3. S. Chakravarty, R.G. Andrews, P.C. Patnaik, and A.K. Koul, The Effect of Surface Modification on Fretting Fatigue in Ti Alloy Turbine Components, *JOM*, vol. 47, No. 4, 1995, pp. 31–35.
4. K. Miyoshi, B.A. Lerch, S.L. Draper, and S.V. Raj, Evaluation of Ti-48Al-2Cr-2Nb Under Fretting Conditions, NASA TM-211205, Nov. 2001.
5. J.M. Larsen, B.D. Worth, S.J. Balsone and J.W. Jones: in *Gamma Titanium Aluminides*, Y.W. Kim, R. Wagner, and M. Yamaguchi, eds., TMS, Warrendale, PA, 1995, pp. 821–834.
6. A.F. Madaayag, *Metal Fatigue: Theory and Design*, John Wiley & Sons, NY, 1969, pp. 144–148.
7. J. Denk and S. Amhof, *Fatigue '96*, Proc. 6th Int. Fatigue Congr., G. Lutjering and H. Nowack, eds., Pergamon Press, 1996, vol. III, pp. 1967–1972.
8. F. Guiu, M.J. Reece, and D.A.J. Vaughan, *Cyclic Fatigue in Some Structural Ceramics*, *Fatigue of Advanced Materials*, Eds. R.O. Ritchie et al., MCEP, Birmingham, 1991, pp. 193–210.
9. Y. Mutoh, M. Takahashi, T. Oikawa, H. Okamoto, *Fatigue Crack Growth of Long and Short Cracks in Silicon Nitride*, *Fatigue of Advanced Materials*, Eds. R.O. Ritchie et al., MCEP, Birmingham, 1991, pp. 211–225.
10. M. Okane, T. Satoh, Y. Mutoh, and S. Suzuki, *Fretting Fatigue Behavior of Silicon Nitride*, *Fretting Fatigue*, Eds. R.B. Waterhouse and T. C. Lindley, Mech. Engng. Publ., London, 1994, pp. 363–371.
11. M. Okane, Y. Mutoh, Y. Kishi, and S. Suzuki, *Static and Cyclic Fretting Fatigue Behavior of Silicon Nitride*, *Fatigue Fract. Engng. Mater. Struct.*, 19, (12), 1996, pp. 1493–1504.
12. E.J. Dollay, N.E. Ashbaugh, and B.D. Worth, *Isothermal High-Cycle-Fatigue of a Ti-46.6Al-3.0Nb-2.1Cr-0.2W (at. %) Gamma Titanium Aluminide*, Proc. of Fatigue '96, Berlin, Pergamon, 1996, vol. III, pp. 1755–1760.
13. T. Hansson, M. Kamaraj, Y. Mutoh, and B. Pettersson, *High Temperature Fretting Fatigue Behavior in an XDTM γ -Base TiAl*, *Fretting Fatigue: Current Technology and Practices*, ASTM STP 1367, D.W. Hoepfner, V. Chandrasekaran, and C.B. Elliot III, Eds., American Society for Testing and Materials, West Conshohocken, PA, 2000, pp. 65–79.

REPORT DOCUMENTATION PAGE			<i>Form Approved</i> <i>OMB No. 0704-0188</i>	
Public reporting burden for this collection of information is estimated to average 1 hour per response, including the time for reviewing instructions, searching existing data sources, gathering and maintaining the data needed, and completing and reviewing the collection of information. Send comments regarding this burden estimate or any other aspect of this collection of information, including suggestions for reducing this burden, to Washington Headquarters Services, Directorate for Information Operations and Reports, 1215 Jefferson Davis Highway, Suite 1204, Arlington, VA 22202-4302, and to the Office of Management and Budget, Paperwork Reduction Project (0704-0188), Washington, DC 20503.				
1. AGENCY USE ONLY (Leave blank)		2. REPORT DATE August 2002	3. REPORT TYPE AND DATES COVERED Technical Memorandum	
4. TITLE AND SUBTITLE Preliminary Study on Fatigue Strengths of Fretted Ti-48Al-2Cr-2Nb			5. FUNDING NUMBERS WU-708-24-13-00	
6. AUTHOR(S) Kazuhisa Miyoshi, Bradley A. Lerch, and Susan L. Draper				
7. PERFORMING ORGANIZATION NAME(S) AND ADDRESS(ES) National Aeronautics and Space Administration John H. Glenn Research Center at Lewis Field Cleveland, Ohio 44135-3191			8. PERFORMING ORGANIZATION REPORT NUMBER E-13139	
9. SPONSORING/MONITORING AGENCY NAME(S) AND ADDRESS(ES) National Aeronautics and Space Administration Washington, DC 20546-0001			10. SPONSORING/MONITORING AGENCY REPORT NUMBER NASA TM-2002-211718	
11. SUPPLEMENTARY NOTES Responsible person, Kazuhisa Miyoshi, organization code 5160, 216-433-6078.				
12a. DISTRIBUTION/AVAILABILITY STATEMENT Unclassified - Unlimited Subject Category: 26 Available electronically at http://gltrs.grc.nasa.gov This publication is available from the NASA Center for AeroSpace Information, 301-621-0390.			12b. DISTRIBUTION CODE	
13. ABSTRACT (Maximum 200 words) The fatigue behavior (stress-life curve) of gamma titanium aluminide (Ti-48Al-2Cr-2Nb, atomic percent) was examined by conducting two tests: first, a fretting wear test with a fatigue specimen in contact with a typical nickel-based superalloy contact pad in air at temperatures of 296 and 823 K and second, a high-cycle fatigue test of the prefretted Ti-48Al-2Cr-2Nb fatigue specimen at 923 K. Reference high-cycle fatigue tests were also conducted with unfretted Ti-48Al-2Cr-2Nb specimens at 923 K. All Ti-48Al-2Cr-2Nb fatigue specimens were machined from cast slabs. The results indicate that the stress-life results for the fretted Ti-48Al-2Cr-2Nb specimens exhibited a behavior similar to those of the unfretted Ti-48Al-2Cr-2Nb specimens. The values of maximum stress and life for the fretted specimens were almost the same as those for the unfretted specimens. The resultant stress-life curve for the unfretted fatigue specimens was very flat. The flat appearance in the stress-life curve of the unfretted specimens is attributed to the presence of a high density of casting pores. The fatigue strengths of both the fretted and unfretted specimens can be significantly affected by the presence of this porosity, which can decrease the fatigue life of Ti-48Al-2Cr-2Nb. The presence of the porosity made discerning the effect of fretting damage on fatigue strength and life of the specimens difficult.				
14. SUBJECT TERMS Materials			15. NUMBER OF PAGES 21	
			16. PRICE CODE	
17. SECURITY CLASSIFICATION OF REPORT Unclassified	18. SECURITY CLASSIFICATION OF THIS PAGE Unclassified	19. SECURITY CLASSIFICATION OF ABSTRACT Unclassified	20. LIMITATION OF ABSTRACT	